Angiotensin II induces reactive oxygen species, DNA damage, and T-cell apoptosis in severe COVID-19

Lucy Kundura, Sandrine Gimenez, Renaud Cezar, Sonia André, Mehwish Younas, Yea-Lih Lin, Pierre Portalès, Claire Lozano, Charlotte Boullé, Jacques Reynes, et al.

Angiotensin II induces reactive oxygen species, DNA damage, and T cell apoptosis in severe COVID-19

Lucy KUNDURA[1], Sandrine GIMENEZ[1], Renaud CEZAR[2], Sonia ANDRÉ[3], Mehwish YOUNAS[1], Yea-Lih LIN[1], Pierre PORTALES[4], Claire LOZANO[4], Charlotte BOULLE[5], Jacques REYNES[5], Thierry VINCENT[4], Clément METTLING[1], Philippe PASERO[1], Laurent MULLER[6], Jean-Yves LEFRANT[6], Claire ROGER[6], Pierre-Géraud CLARET[7], Sandra DUVNJAK[8], Paul LOUBET[9], Albert SOTTO[9], Tu-Anh TRAN[10], Jérôme ESTAQUIER[3,11]†, Pierre CORBEAU[1,2]†*

[1]Institute of Human Genetics, UMR9002, CNRS and Montpellier University; Montpellier, France.

[2]Immunology Department, Nîmes University Hospital; Nîmes, France.

[3]INSERM U1124, Université de Paris; Paris, France.

[4]Immunology Department, Montpellier University Hospital; Montpellier, France.

[5]Infectious diseases Department, Montpellier University Hospital; Montpellier, France.

[6]Surgical Intensive Care Department, Nîmes University Hospital; Nîmes, France.

[7]Medical and Surgical Emergency Department, Nîmes University Hospital; Nîmes, France.

[8]Gerontology Department, Nîmes University Hospital; Nîmes, France.

[9]Infectious diseases Department, Nîmes University Hospital; Nîmes, France.

[10]Pediatrics Department, Nîmes University Hospital; Nîmes, France.

[11]Laval University Research Center; Quebec City, Quebec, Canada.

*Corresponding author: Pierre Corbeau; address, Institute of Human Genetics, 141 rue de la Cardonille, 34396 Montpellier cedex 5, France; phone number, +33-434359932; fax number, +33-434359901; e-mail address: pcorbeau@igh.cnrs.fr.

† These authors contributed equally to this work.

Funding. This study was supported by the University Hospital of Nîmes grant NIMAO/2020/COVID/PC-01 (PC)**,** the Fondation Recherche Médicale and the Agence Nationale de Recherche grant 216261 (JE) and an AbbVie grant (PC).

Word count. 4552.

Abstract

Background. Lymphopenia is predictive of survival in Coronavirus disease 2019 (COVID-19) patients.

Objective. The aim of this study was to understand the cause of a lymphocyte count drop in severe forms of SARS-CoV-2 infection.

Methods. Monocytic production of reactive oxygen species (ROS) and T cell apoptosis were measured by flow cytometry, DNA damage in peripheral mononuclear blood cells (PBMCs) by immunofluorescence, and Angiotensin II (AngII) by ELISA in SARS-CoV-2-infected patients upon admission to Intensive Care Units (ICU, n=29) or non-ICU (n=29), and in age- and sex-matched healthy controls.

Results. We show that the monocytes of certain COVID-19 patients spontaneously released ROS able to induce DNA damage and apoptosis in neighboring cells. Of note, high ROS production was predictive of death in ICU patients. Accordingly, in most patients, we observed the presence of DNA damage in up to 50% of their PBMCs, and T-cell apoptosis. Moreover, the intensity of this DNA damage was linked to lymphopenia. SARS-CoV-2 is known to induce the internalization of its receptor, Angiotensin Converting Enzyme 2, a protease able to catabolize AngII. Accordingly, we observed in certain COVID-19 patients high plasma levels of AngII. Looking for the stimulus responsible for their monocytic ROS production, we unveiled that AngII triggers ROS production by monocytes via Angiotensin receptor I. ROS released by AngII-activated monocytes induced DNA damage and apoptosis in neighboring lymphocytes.

Conclusion. We conclude that T cell apoptosis provoked via DNA damage due to the release of monocytic ROS could play a major role in COVID-19 pathogenesis.

Clinical implication. Unveiling this new pathogenic pathway opens up new therapeutic possibilities for COVID-19.

Capsule summary. SARS-CoV-2 may trigger a cascade of events resulting in programmed T cell death and severe COVID-19 which may be prevented by an Angiotensin receptor I antagonist and/or an antioxidant.

Key words. SARS-CoV-2, ACE2, oxidative stress, antioxidant, Angiotensin II receptor, DNA oxidation, programmed cell death, lymphopenia.

Running title: DNA damage and T cell apoptosis in COVID-19

Abbreviations. SARS-CoV-2, severe acute respiratory syndrome coronavirus 2; COVID-19, coronavirus disease 2019; ACE2, Angiotensin-converting enzyme 2; ICU, Intensive Care Units; HD, healthy donor; RNA, ribonucleic acid; NADP, nicotinamide adenine dinucleotide phosphate; ROS, reactive oxygen species; AngII, Angiotensin II; PBMCs, peripheral mononuclear blood cells; DCFH-DA, dichloro-dihydro-fluorescein diacetate; DPI, diphenyleneiodonium; AU, arbitrary unit; NAC, N-acetylcysteine; AT1, Angiotensin receptor 1; PaO2, arterial oxygen tension; mAb, monoclonal antibody; FBS, fetal bovine serum; LPS, lipopolysaccharide.

Conflicts of interests. Authors declare that they have no conflicts of interests.

INTRODUCTION

COVID-19 is an infectious disease caused by severe acute respiratory syndrome coronavirus 2 (SARS-CoV-2). The most severe forms of COVID-19 are due to acute lung damage which is strongly linked to hyperactivation of the immune system (1). A hallmark of critical COVID-19 is lymphopenia (2), observed in up to 63% of COVID-19 patients, and predictive of an unfavorable outcome (3). Yet, the cause of peripheral blood T-cell, B-cell, and NK-cell loss remains unclear. Indeed, this loss may be the consequence of a decrease in lymphocyte production, the trapping of these cells in the respiratory tract and/or a high rate of lymphocyte death. As lymphocyte counts are strongly predictive of survival, understanding the causes of lymphopenia is of major importance.

Various ribonucleic acid (RNA) viruses have been reported to induce ROS production and antioxidant system depletion. For instance, the influenza virus increases the level of ROS production in the host cells and decreases the concentration of antioxidants (4). Moreover, the oxidative stress provoked by the virus is responsible for lung damage that may be prevented by antioxidants or by targeting nicotinamide adenine dinucleotide phosphate (NADPH) oxidase-2 (4). Likewise, respiratory syncytial virus infection causes ROS expression (5) and decreases the expression of antioxidant genes, contributing to bronchiolitis (6). SARS-CoV-1 modifies the oxidoreductase system of the mitochondria, via an interaction between its non-structural protein 10 and cytochrome oxidase II (7). In line with this mechanism, oxidative stress has been reported in the lungs of SARS-CoV-1-infected mice (8). Likewise, SARS-CoV-2-infected monocytes overproduce mitochondrial ROS, and an increased expression of oxidative stress-associated genes has been observed in monocytes of bronchoalveolar fluid from COVID-19 patients (9). In the peripheral blood of these patients, markers of NADPH oxidase-2 activation (10), impaired

antioxidant activity (11) and oxidative stress (12) have been revealed as possibly being linked to the severity of the disease.

As ROS can cause DNA damage resulting in apoptosis (13), we analyzed the level of monocytic ROS production in COVID-19 patients at different stages, as well as its causes and consequences.

MATERIALS AND METHODS

Study design. This is an observational, monocentric, case-control study. Adults with positive naso-pharyngeal swabs for SARS-CoV-2 RNA by RT-PCR were consecutively recruited at the Nîmes University Hospital. Patients were either recruited on the day of their admission to an intensive care unit (ICU) for oxygen saturation <90% in ambient air or <95% with 5L/mn of oxygenotherapy and/or arterial oxygen tension (PaO2) of less than 60 mm Hg or upon admission to the Tropical and Infectious Diseases Department (non-ICU) for oxygen saturation <96% in ambient air. No outlier was excluded. All the replicates were biological. This study was approved by the French Ethics Committee, Île-de-France 1. All patients had provided written informed consent, and the trial was registered (Eudract/IDRCB 2020-A00875-34 and ClinicalTrials NCT04351711).

Cell-sorting and co-culture. Monocytes were sorted from peripheral mononuclear blood cells (PBMCs) using CD14-coated microbeads (Miltenyi Biotech). Cells, pre-incubated or not with diphenyleneiodonium (DPI) or N-acetylcysteine (NAC) for 3 hours at 37°C, were washed twice and cocultured in 1µm pore-size inserts with BJ cells (fibroblasts established from skin, ATCC CRL-2522) placed on coverslips in 24-well companion plates. PBMCs or monocytes and BJ cells were co-cultured in 2:1 ratio in 1:1 DMEM and RPMI culture media supplemented with 10% heat-inactivated fetal bovine serum (FBS) for 3 days. Camptothecin (10µM) was used on BJ cells for 45 min at 37°C. Lipopolysaccharide (LPS, 1µg/ml) or Angiotensin II (AngII, 75pM) was added to the cells in 500µl final volume of RPMI without serum and incubated at 37°C for 30 minutes. Cells were washed and fixed for further staining.

Immunofluorescence. PBMC adherence on coverslips was obtained by using 20 µg/ml of poly-lysine in serum-free RPMI for 2 hours at room temperature. Coverslips with cocultured BJ cells

were washed twice, fixed with 2% paraformaldehyde in PBS for 10 minutes, rinsed again with PBS, and permeabilized with PBS containing 0.1% Triton-X-100 for 10 minutes at room temperature. Thereafter, coverslips were washed and blocked with PBS containing 10% FBS for 30 minutes. Cells were then incubated with anti-γ-H2AX (Millipore, 1/500) for 1 hour or anti-53BP1 (Millipore, 1/300) monoclonal antibodies (mAb) in PBS with 10% FBS. Coverslips were rinsed three times with PBS and incubated with AF 546 anti-mouse IgG1 (Invitrogen, 1/2000) secondary antibody for 45 minutes in PBS with 10% FBS at room temperature. After washing with PBS, DNA was counter stained with DAPI (Sigma-Aldrich) for 5 minutes, and coverslips were mounted in fluorescence mounting medium (Prolong gold, Invitogen). Slides were kept overnight at 20°C in a dark room. Images were obtained with a Zeiss ApoTome fluorescence microscope (63X magnification and 1.4 numerical aperture for BJ cells, 100X magnification and 1.46 numerical aperture for PBMC) with supporting software, and analyzed on Image J and FIJI software systems.

Flow Cytometry. The monoclonal antibodies used for cell surface staining were: CD3-APCA750, CD14-PE, CD16-APC, CD4-APC (Beckman Coulter), CD3-BV421 and CD3-AF700 (Biolegend). Annexin-V-PE (Biolegend) was used according to manufacturer's guidelines. For ROS quantification, 10^6 PBMCs were resuspended in 1μM dichloro-dihydro-fluorescein diacetate (DCFH-DA) for 25min at room temperature. Data were acquired on a Navios flow cytometer (Beckman Coulter) from 20,000 gated events per sample and on a MACSQuant analyser 10 (Miltenyi Biotech), and analyzed using Kaluza software.

ELISA. AngII concentrations were determined using the Angiotensin II ELISA kit (Enzo Life Sciences).

Statistical analyses. No data pre-processing was performed. Statistical analyses and graphical presentations were computed with GraphPad Prism version 6. D'Agostino and Pearson normality test was performed. Differences between two groups were analyzed using two-sided unpaired student's *t* test or Mann-Whitney test as appropriate. Differences between more than two groups were analyzed using one-way ANOVA, Welch ANOVA or Kruskal-Wallis test as appropriate. We used a two-sided Spearman rank test to evaluate correlations. A p value of <0.05 was considered statistically significant.

RESULTS

Patient enrollment

We enrolled 29 PCR-positive SARS-CoV-2-infected patients upon admission to ICUs for an oxygen saturation of less than 90% and/or PaO2 below 60 mmHg in room air, or an oxygen saturation of less than 95% while receiving 5L/min of oxygen. We also recruited 29 PCR-positive SARS-CoV-2-infected patients upon admission to the Infectious Diseases Department (non-ICU) for an oxygen saturation of less than 96% in room air and/or deterioration in their general condition. Age- and sex-matched healthy donor (HDs: age range, 28 to 95 years) were used as negative controls. The bioclinical characteristics of these patients are shown in Table 1.

Table 1. Bioclinical characteristics of the patients enrolled

		Non-ICU patients (n=29)	ICU patients (n=29)	non-ICU vs ICU
Age (years)	Mean (SD) Range	66.1 (20.9) 29.0-96.0	69.3 (13.5) 43.0-95.0	p = 0.702
Gender: Females Males	 n (%) n (%)	 16 (55) 13 (45)	 13(45) 16 (55)	p = 0.600
Any comorbidity	n (%)	12 (40)	12 (41)	p = 0.594
Diabetes	n (%)	7 (23)	7 (24)	p = 0.762
Cancer	n (%)	4 (13)	2 (7)	p = 0.783
Autoimmune disease	n (%)	1 (3)	0 (0)	p = 0.999
Chronic kidney failure	n (%)	0 (0)	2 (7)	p = 0.202
Duration of symptomatology (days)	Mean (SD)	6.8 (9.4)	11.8 (7.2)	p < 0.001
C-reactive protein (mg/L, normal range 0.9-1.8)	Mean (SD)	56.8 (68.1)	115.0 (81.3)	p = 0.003
Lactate dehydrogenase (IU/L, normal range 135-214)	Mean (SD)	214.8 (49.9)	416.4 (177.3)	p < 0.001
Absolute lymphocyte count ($x10^9$/L, normal range 0.9-1.8)	Mean (SD)	1.30 (0.53)	0.88 (0.59)	p = 0.004
Absolute monocyte count ($x10^9$/L, normal range 0.9-1.8)	Mean (SD)	0.70 (0.36)	0.46 (0.27)	p = 0.010

Monocytes from COVID-19 patients overproduce ROS

To test whether monocytes from COVID-19 patients produced ROS, we labeled the peripheral PBMCs of SARS-CoV-2-infected individuals with DCFH-DA, which reacts with ROS to give a fluorescent product. Figure 1A shows that monocytes from HDs become fluorescent when they are incubated with DCFH-DA and exposed to LPS, used as a positive control. This ROS

production was prevented by pre-incubation with the NADPH oxidase inhibitor diphenyleneiodonium (DPI, Fig. 1A). By contrast, the spontaneous fluorescence of monocytes from HDs incubated with DCFH-DA was not reduced in the presence of DPI (Fig. 1A). Monocytes from certain COVID-19 patients became more fluorescent than monocytes from HDs after being exposed to DCFH-DA (Fig. 1B and 1C). Figure 1C shows the intensity of spontaneous monocytic ROS production in HDs, ICU and non-ICU patients. Non-ICU patients produced more ROS than HDs (22.2 ± 4.5 vs. 17.2 ± 4.6 mean ± standard deviation (SD) arbitrary units of mean fluorescence intensity (AU), *t* test p = 0.004) whereas ICU patients did not (16.4 ± 3.9 vs. 17.2 ± 4.6 mean ± SD AU, *t* test p = 0.855). Yet, the ICU patients who survived presented lower monocytic ROS production than those who did not (15.6 ± 3.4 vs. 19.6 ± 4.1 mean ± SD AU, *t* test p = 0.021, Fig. 1D). To identify the monocyte subpopulations responsible for ROS production, we labeled the PBMCs exposed to DCFH-DA with anti-CD14 and anti-CD16 antibodies to identify classical (CD14hiCD16lo), intermediate (CD14+CD16+), and alternative (CD14loCD16hi) monocytes (Fig. 1E). Figure 1F shows that the intermediate and classical monocytes produced the highest amount of ROS. Compared with ICU, non-ICU participants had a higher percentage of intermediate monocytes (20.7 ± 13.8 vs. 10.7 ± 16.2 median ± interquartile range (IQR), Mann-Whitney p = 0.055, Fig. 1G). Logically, the proportions of intermediate monocytes and ROS-producing monocytes were correlated in COVID-19 patients (r = 0.373, p = 0.004, Fig. 1H).

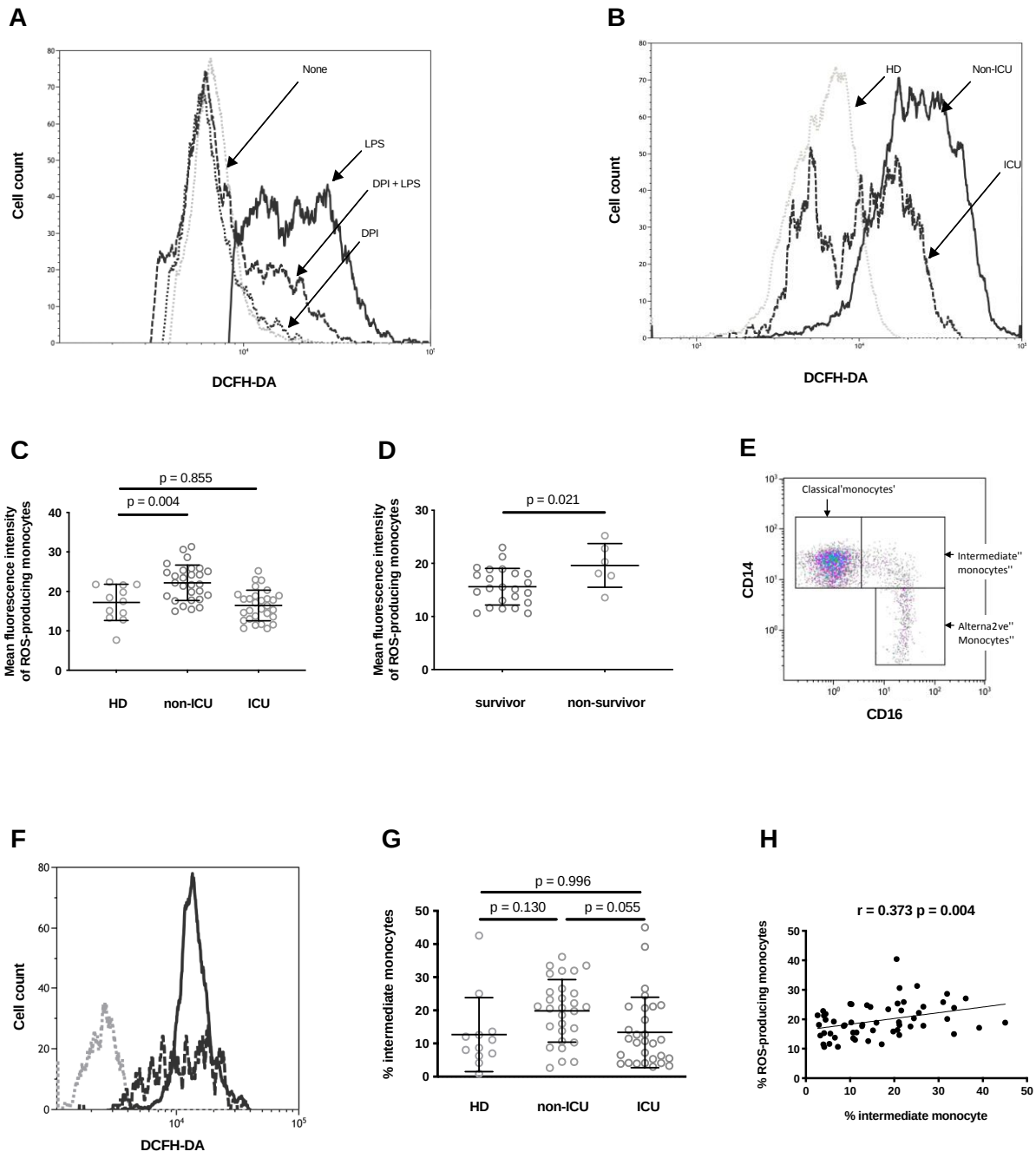

Figure 1. The monocytes from certain COVID-19 patients spontaneously produce ROS. (A) Fluorescence in monocytes from a healthy donor, pre-incubated (DPI + LPS, ---) or not (LPS, —) with DPI, exposed to DCFH-DA, and stimulated with lipopolysaccharide. As negative controls, fluorescence in the same monocytes pre-incubated (DPI, ···) or not (None, ···) with NADPH oxidase inhibitor DPI and exposed to DCFH-DA was analyzed. (B) Fluorescence in monocytes from a healthy donor (HD, ···), a non-ICU patient (non-ICU, —), and an ICU patient (ICU, ---) exposed to DCFH-DA. (C) Mean fluorescence intensity of ROS-producing monocytes from healthy

donors (HD), non-ICU patients (non-ICU), and ICU patients (ICU) exposed to DCFH-DA. One-way ANOVA test $p < 0.001$. (D) Mean fluorescence intensity of ROS-producing monocytes from ICU patients who survived or not. (E) Identification of the classical, intermediate, and alternative monocyte subpopulations by flow cytometry. (F) Fluorescence in CD14hiCD16lo (---), CD14+CD16+ (—), and CD14loCD16hi (¨) monocytes from an ICU patient exposed to DCFH-DA. (G) Percentages of CD14-CD16+ monocytes circulating in healthy (HDs), ICU and non-ICU donors. One-way ANOVA test $p = 0.032$. (H) Correlation between the proportions of intermediate and ROS-producing monocytes in ICU and non-ICU patients.

Monocytes from COVID-19 patients induce DNA damage via ROS

ROS can oxidize proteins, lipids or DNA. We searched for the effect of monocytic ROS production on the DNA of bystander cells. For this purpose, we probed the presence of the phosphorylated form of the histone variant H2AX (γ–H2AX), a hallmark of chromosome breaks and DNA replication stress (14), in primary BJ fibroblasts co-cultured with PBMCs from COVID-19 patients. In this assay, PBMCs were co-cultured in transwells, i.e. with no cell-to-cell contact with BJ cells. Camptothecin, a topoisomerase I inhibitor which induces replication-dependent DNA lesions, was used as a positive control, whereas PBMCs from healthy donors were included as negative controls. We found that PBMCs in 8 out of the 25 patients we tested (32%), induced γ–H2AX nuclear foci in bystander BJ cells as exemplified in Figure 2A and 2B. Figure 2C shows that the formation of these foci was prevented by pre-incubating PBMCs with the ROS scavenger, NAC, or the NADPH oxidase inhibitor, DPI. This establishes that the γ–H2AX foci are indeed induced by ROS. To make really sure that the sources of DNA cells damaging ROS were monocytes, we repeated the experiment after depleting patient PBMCs of monocytes using CD14-coated magnetic beads. Figure 2D shows that, whereas PBMCs and

monocytes from the patient we analyzed induced DNA damage, monocyte-depleted PBMCs from the same patient did not.

PBMC DNA damage results in T-cell apoptosis during severe SARS-CoV-2 infection

ROS-induced DNA damage may provoke apoptosis (13). Therefore, we tested whether co-culturing with COVID-19 PBMCs might trigger apoptosis in HD PBMCs. Indeed, HD T-cells presented more phosphatidylserine at their surface, a marker of apoptosis, as measured by Annexin V labelling on day 6 when they were exposed to COVID-19 PBMCs able to induce DNA damage than when they were exposed to another healthy volunteer PBMCs (15.0 ± 1.5 vs. 10.8 ± 1.7 % mean ± SD, *t* test p = 0.034, Fig. 2E). This programmed cell death provoked by COVID-19 PBMCs was entirely mediated by ROS, since the presence of NAC reduced apoptosis to the background level observed in the presence of HD PBMCs (11.8 ± 1.6 vs. 10.8 ± 1.7 % mean ± SD, *t* test p = 0.939, Fig. 2E). By contrast, co-culturing with COVID-19 PBMCs unable to induce DNA damage or with HD PBMCs resulted in the same level of apoptosis (11.7 ± 2.1 vs. 10.8 ± 1.7 % mean ± SD, *t* test p = 0.959, Fig. 2E). As a positive control, we used LPS-stimulated PBMCs, which triggered apoptosis in HD PBMCs (17.6 ± 1.6 vs 10.8 ± 1.7 % mean ± SD, *t* test p = 0.001, Fig. 2E). We obtained the same results when we co-cultured purified COVID-19 monocytes able to cause DNA damage with HD PBMCs (Fig. 2F). The monocytes of a patient (patient 3) known to induce γ–H2AX foci in neighbouring cells provoked apoptosis in co-cultured PBMCs (6.8 ± 3.4% vs. 3.7 ± 2.8% mean ± SD, *t* test p = 0.027), prevented by DPI (4.4 ± 2.1% vs. 3.7 ± 2.8% mean ± SD, *t* test p = 0.980), whereas monocytes of a patient (patient 4) unable to induce γ–H2AX foci in neighbouring cells did not (4.3 ± 2.1% vs. 3.7 ± 2.8% mean ± SD, *t* test p = 0.972).

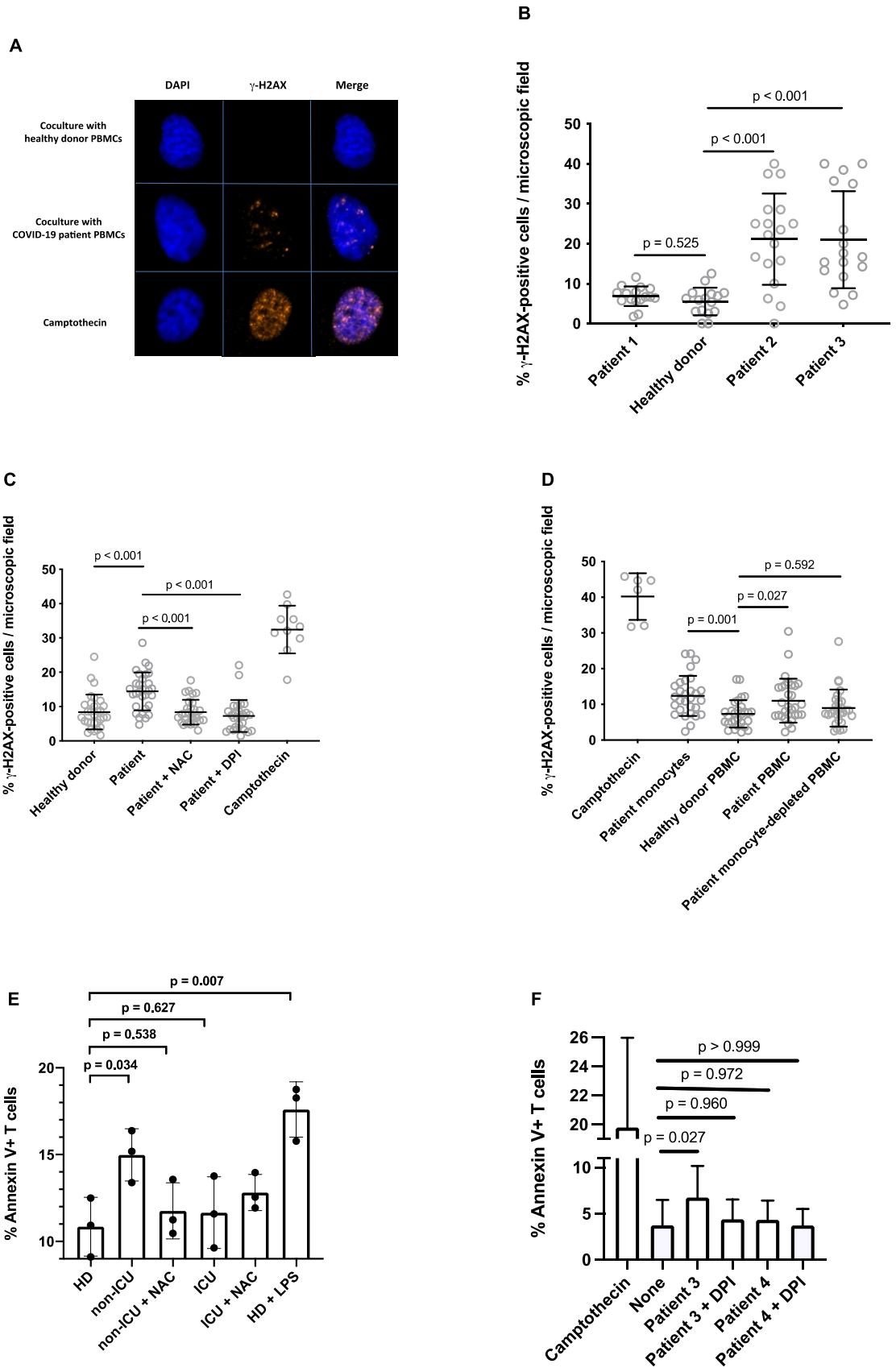
A
DAPI
γ-H2AX
Merge
Coculture with healthy donor PBMCs
Coculture with COVID-19 patient PBMCs
Camptothecin
B
% γ-H2AX-positive cells / microscopic field
p < 0.001
p < 0.001
p = 0.525
Patient 1
Healthy donor
Patient 2
Patient 3
C
% γ-H2AX-positive cells / microscopic field
p < 0.001
p < 0.001
p < 0.001
Healthy donor
Patient
Patient + NAC
Patient + DPI
Camptothecin
D
% γ-H2AX-positive cells / microscopic field
p = 0.592
p = 0.027
p = 0.001
Camptothecin
Patient monocytes
Healthy donor PBMC
Patient PBMC
Patient monocyte-depleted PBMC
E
% Annexin V+ T cells
p = 0.007
p = 0.627
p = 0.538
p = 0.034
HD
non-ICU
non-ICU + NAC
ICU
ICU + NAC
HD + LPS
F
% Annexin V+ T cells
p > 0.999
p = 0.972
p = 0.960
p = 0.027
Camptothecin
None
Patient 3
Patient 3 + DPI
Patient 4
Patient 4 + DPI

Figure 2. COVID-19 patient monocytes may induce DNA damage via ROS. (A) Detection of γ–H2AX foci by immunofluorescence in BJ cells co-cultured with PBMCs from a healthy donor or from a COVID-19 patient. Healthy donor's PBMCs treated with camptothecin were used as positive controls. (B) Quantification of the γ–H2AX foci induced in BJ fibroblasts by PBMCs from COVID-19 patients. The proportion of BJ cells presenting at least 5 foci per nucleus was quantified under microscopy. Each point represents one microscope field. Welch ANOVA test $p < 0.001$. (C) γ–H2AX foci induced in BJ cells by COVID-19 patient's PBMCs are prevented by pre-incubating PBMCs with N-acetylcysteine (NAC) or diphenyleneiodonium (DPI). Each point represents one microscope field. Kruskal-Wallis test $p < 0.001$. (D) Monocytes isolated from the PBMCs of a COVID-19 patient are able to induce DNA damage in BJ cells. The ability to induce γ–H2AX foci in the BJ fibroblasts of PBMCs from a COVID-19 patient, of the same PBMCs depleted of monocytes, and of monocytes isolated from these PBMCs was tested. Each point represents one microscope field. Kruskal-Wallis test $p < 0.001$. (E) Intensity of phosphatidylserine expression at the surface of healthy donor PBMCs cocultured with non-ICU PBMCs able to induce DNA damage treated (non-ICU + NAC) or not (non-ICU) with N-acetylcysteine, or with ICU PBMCs unable to induce DNA damage treated (ICU + NAC) or not (ICU) with N-acetylcysteine, as detected by flow cytometry at day 6. Healthy donor PBMCs co-cultured with another healthy donor PBMCs (HD) or treated with lipopolysaccharide (HD + LPS) were used as negative and positive controls, respectively. One-way ANOVA test $p = 0.002$. (F) Intensity of phosphatidylserine expression at the surface of healthy donor PBMCs cocultured with COVID-19 monocytes able (patient 3) or not (patient 4) to induce DNA damage and treated (+ DPI) or not with DPI, as detected by flow cytometry at day 6. Camptothecin was used as a positive control.

COVID-19 patient PBMCs present DNA damage

As the monocytes of certain COVID-19 patients release ROS which are able to cause DNA damage to neighboring cells, we analyzed whether the PBMCs of these patients presented DNA damage. To do this, we looked for the presence of γ–H2AX nuclear foci in their PBMCs. Figure 3A shows an example of a COVID-19 patient whose PBMCs harbor such DNA damage markers. Globally, the proportion of DNA-damaged PBMCs was higher in the 19 non-ICU patients (9.7 ±

4.0 % vs. 5.8 ± 2.9 % median ± IQR, Mann-Whithney p = 0.003), and the 28 ICU patients (10.0 ± 8.4 % vs. 5.8 ± 2.9 % median ± IQR, Mann-Whithney p < 0.001) than in age-matched healthy donors we analyzed (Fig. 3B). COVID-19 patient PBMCs also harboured DNA double-strand breaks, as revealed by the labelling with an antibody specific for 53BP1, a protein known to aggregate at double-strand ends (15). In the example shown in Figure 3C, 16.8 ± 3.4 % of the patient PBMCs presented 53BP1 foci, a higher proportion than in the healthy donor (6.9 ± 1.6 % mean ± SD, *t* test p = 0.011). Next, we quantified CD4+ T-cell and CD8+ T-cell apoptosis in the participant peripheral blood. Figure 3D shows that Annexin V expression at the surface of both lymphocyte subpopulations, particularly on CD8+ T-cells, was more frequent in COVID-19 patients than in controls. We also tested whether the phenomenon we describe could result in lymphopenia in COVID-19 patients. To this aim, we looked for a correlation between the intensity of DNA damage in PBMCs and lymphopenia. As shown in Figure 3E, we observed an inverse correlation between the percentage of PBMCs with γ–H2AX foci and lymphocyte count in the patients and healthy volunteers we analyzed (r = -0.341, p = 0.025).

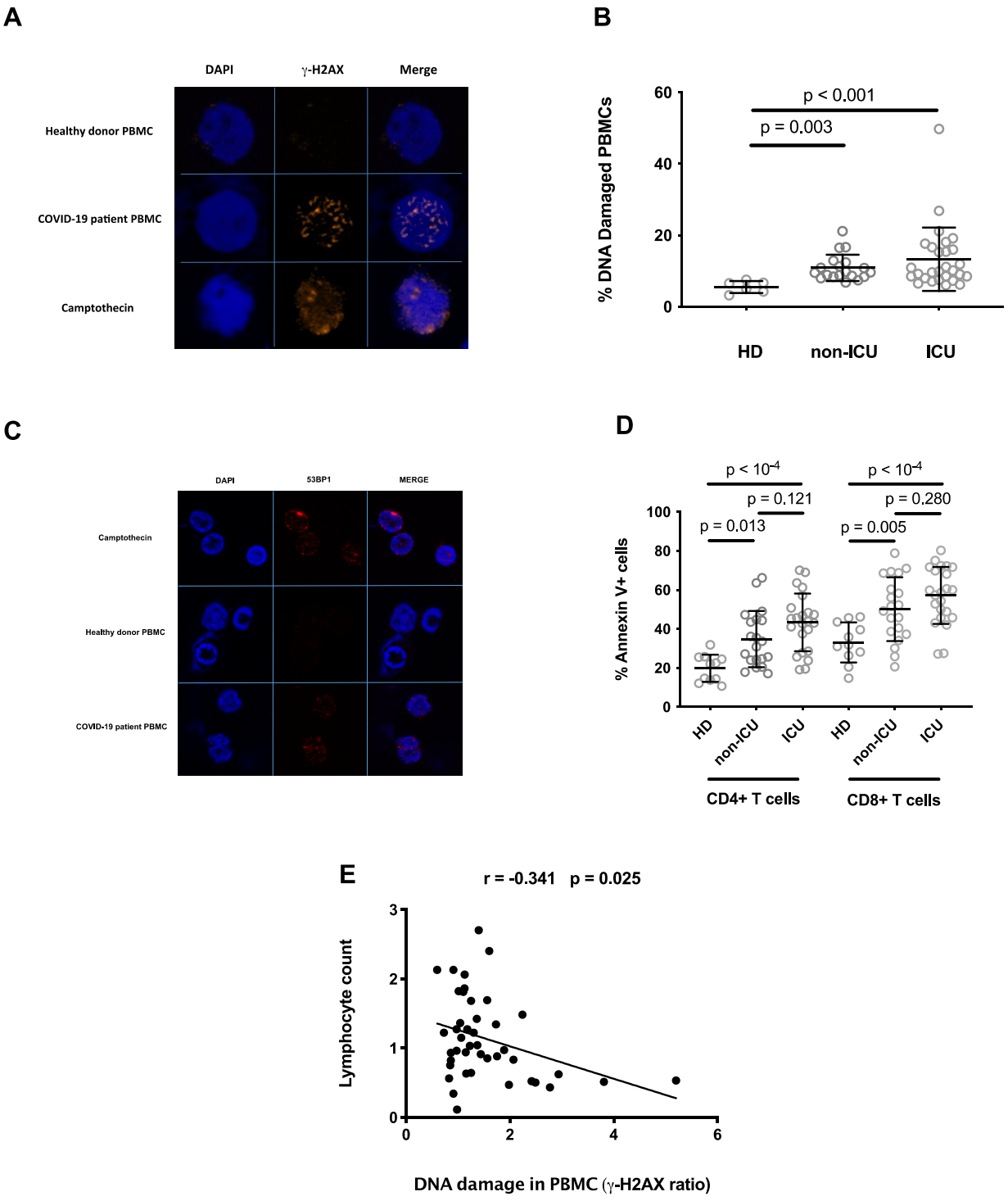

290
291

292
293
294

Figure 3. DNA damage in COVID-19 PBMCs. (A) PBMCs from a COVID-19 patient whose monocytes induce DNA damage in bystander BJ cells spontaneously present with γ–H2AX foci. PBMCs from a healthy donor treated or not with camptothecin were used as positive and negative controls, respectively. (B) Percentages of PBMCs harboring γ–H2AX foci in healthy donors (HD), non-ICU patients (non-ICU), and ICU patients (ICU). Kruskal-Wallis test $p = 0.002$. (C) PBMCs from a COVID-19 patient whose monocytes induce DNA damage in bystander BJ cells spontaneously present with 53BP1 foci. PBMCs from a healthy donor treated or not with camptothecin were used as positive and negative controls, respectively. (D) Annexin V expression on peripheral blood CD4+ T-cells and CD8+ T-cells of healthy donors (HD), non-ICU patients (non-ICU), and ICU patients (ICU). One-way ANOVA test $p < 0.001$ for CD4+ T-cells and $p < 0.001$ for CD8+ T-cells. (E) Correlation between the intensity of DNA damage in PBMC and lymphocyte counts. The intensity of DNA damage in PBMCs is expressed as the ratio (% patient PBMCs presenting γ–H2AX foci) : (% HD PBMCs presenting γ–H2AX foci).

Angiotensin II induces monocytic ROS production

SARS-CoV-2 downregulates the cell surface expression of Angiotensin-converting enzyme 2 (ACE2), its main receptor, via ACE2 co-internalization and cleavage by the serine protease TMPRSS2 (16). Knowing that ACE2 converts AngII into Angiotensin 1-7, this should result in an increase in AngII concentration (16). As AngII has been shown to induce ROS production in human mesangial cells (17), we tested whether this peptide was also able to provoke the release of ROS by human monocytes. Indeed, we observed that, like lipopolysaccharide, AngII increased the fluorescence of HD monocytes preincubated with DCFH-DA (Fig. 4A). This effect was completely prevented by 1-hour preincubation with DPI (91,7 ± 15.3%, Fig. 4B) or the Angiotensin receptor 1 (AT1) antagonist losartan at 10μg/mL (98,7 ± 4.5%, Fig. 4C). Next, we checked to see whether the peripheral blood concentration of AngII was actually high in COVID-19 patients. Figure 4D shows that plasma levels of AngII in non-ICU patients (72.3 ± 68.6 vs. 54.5 ± 73.3 pg/mL median ± IQR , Mann-Whitney test $p = 0.017$), but not in ICU

patients (33.2 ± 31.5 vs. 54.5 ± 73.3 pg/mL median ± IQR , Mann-Whitney test $p > 0.999$) were higher than those of normal volunteers. The lower level of AngII in ICU patients as compared with non-ICU patients might be the consequence of the increase in ACE2 expression reported in severe COVID-19 (18), driven by interferon (19), and/or reoxygenation (20). To test the hypothesis that AngII might be involved in the monocytic ROS overproduction that we had unveiled in certain patients, we looked for a link between AngII plasma levels and the intensity of ROS synthesis in HD, ICU and non-ICU participants. Figure 4E shows a clear correlation between these two parameters ($r = 0.299$, $p = 0.027$). This explains the fact that ROS expression was less intense in ICU patients than in non-ICU patients Thereafter, we checked whether AngII-stimulated monocytes could induce DNA damage in BJ cells. Indeed, this was the case, and the DNA damage was prevented by DPI (Fig. 4F) and the AT1 antagonist losartan (Fig. 4G). We repeated the experiment with HD PBMCs instead of BJ cells (Fig. 4H). Again, we observed that AngII-activated monocytes were able to cause a DNA damage which was prevented by losartan or DPI. Furthermore, circulating levels of AngII strongly correlated with the ability of patient PBMCs to induce DNA damage in BJ cells ($r = 0.704$, $p = 0.005$, Fig. 4I).

T cell surface Fas expression is linked to ROS production

Our data are compatible with a model where ROS-induced DNA damage provokes T cell apoptosis. We have previously observed in severe COVID-19 that programmed T cell death is also linked to T cell surface expression of the death receptor Fas (CD95) (21). ROS are known to increase Fas expression in kidney cells (22), intestinal cells (23), myogenic cells (24), and neurons (25). Conversely, in chronic granulomatous disease, characterized by a defect in ROS production, patients express low T cell surface levels of Fas (26). Therefore, we searched for an

association between monocytic ROS production and Fas expression on T cells in COVID-19 patients. Figure 4J shows a strong link between these two parameters ($r = 0.461$, $p = 0.013$). Thus, ROS released by monocytes could provoke apoptosis in T cells not only by breaking their DNA, but also by inducing Fas expression at their surface.

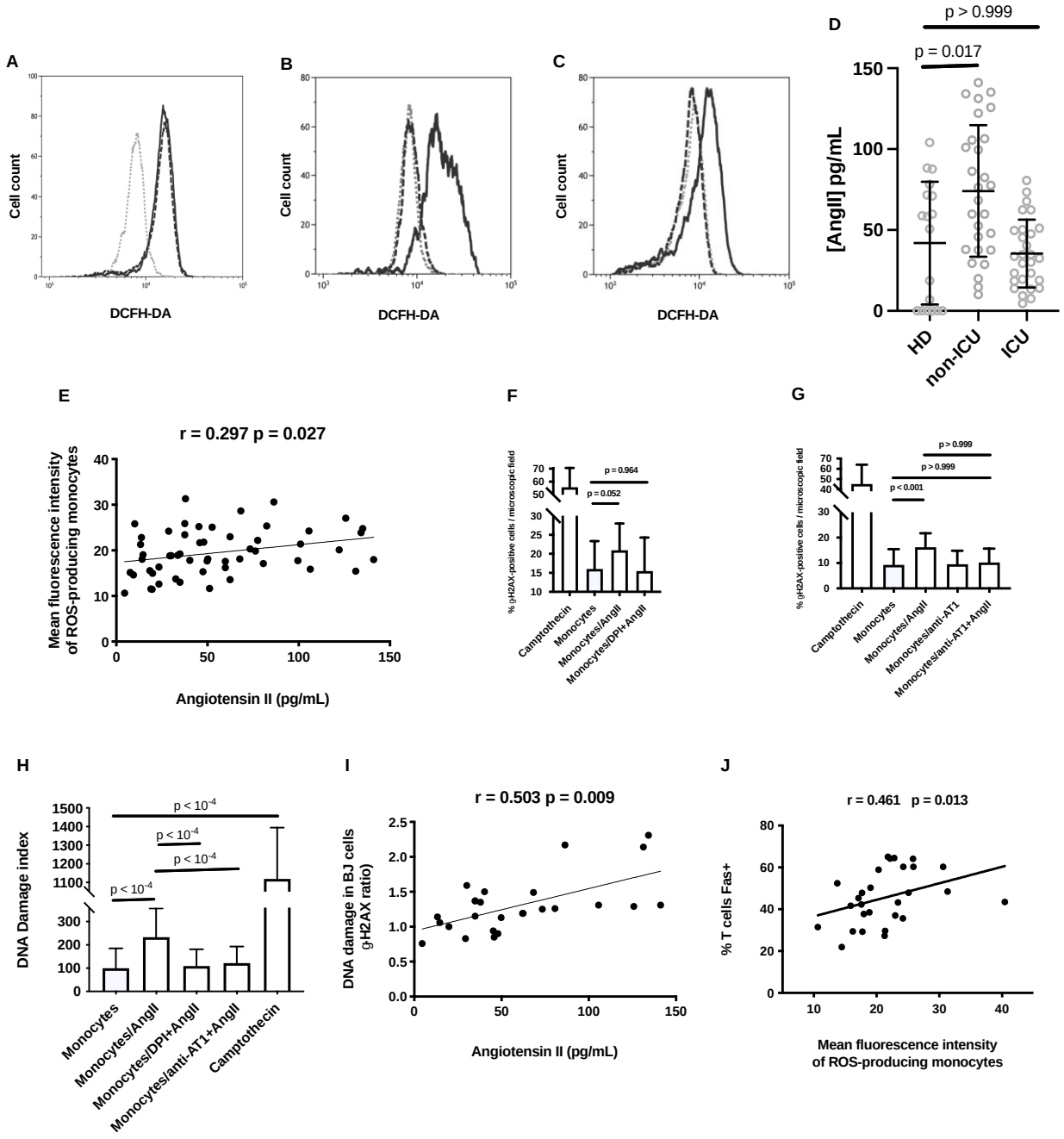

Figure 4. Angiotensin II induces ROS monocytic production and DNA damage. (A) Fluorescence in monocytes from a healthy donor, pre-incubated or not (¨) with LPS (---) or AngII (—), and exposed to DCFH-DA. (B) Fluorescence in monocytes from a healthy donor, pre-incubated or not (¨) with AngII (—) or with DPI and AngII (---), and exposed to DCFH-DA. (C) Fluorescence in monocytes from a healthy donor, pre-incubated or not (¨) with AngII (—), or with losartan and AngII (---), and exposed to DCFH-DA. (D) Plasma levels of AngII in patients and controls. Kruskal-Wallis test $p = 0.001$. (E) Correlation between plasma levels of AngII and mean fluorescence intensity of ROS-producing monocytes exposed to DCFH-DA in patients and controls. (F, G, H) AngII-activated monocytes induce DNA damage in neighbouring cells. Ability of healthy donor monocytes stimulated (Monocytes/AngII) or not (Monocytes) by AngII to cause γ-H2AX foci in bystander BJ cells (F, G) and HD PBMCs (H). The effect or DPI (Monocytes/DPI+AngII, f) or AT1 antagonist (Monocytes/anti-AT1+AngII, g) preincubation on the ability of AngII-stimulated monocytes to induce DNA damage is shown. BJ cells (F, G) or PBMCs (H) exposed to camptothecin were used as a positive control (Camptothecin). F, Welch ANOVA $p < 0.001$; G and H, Kruskal-Wallis test $p < 0.001$. (I) Correlation between plasma levels of AngII and the ability of patient PBMCs to induce γ–H2AX foci in bystander BJ cells. This ability is expressed as the ratio (% BJ cells presenting γ–H2AX foci in presence of patient PBMCs) : (% BJ cells presenting γ–H2AX foci in presence of HD PBMCs). (J) Correlation between mean fluorescence intensity of ROS-producing monocytes exposed to DCFH-DA and the percentage of T lymphocytes expressing Fas.

DISCUSSION

In this study, we discovered a new pathogenic mechanism, DNA damage and T cell surface Fas overexpression due to AngII-driven ROS production by the monocytes of certain COVID-19 patients, and resulting in PBMC apoptosis (Fig. S1). Of note, ICU patients exhibit more T cell apoptosis and lymphopenia than non-ICU patients whereas their plasma level of AngII and their monocytic ROS production are lower. The explanation to this apparent paradox might lie in the delay of a few days between DNA damage and apoptosis (speculative scenario shown in Fig. S2). This delay could be due to the fact that cells first try to repair the damage, and thereafter, in case of failure, trigger apoptosis (27). Accordingly, we observed apoptosis in PBMCs co-cultured with patient monocytes only after 6 days (Fig. 2, E and F). Non-ICU patients are at Day 7 of the disease (Table 1). SARS-CoV-2 has replicated, internalized ACE2, and thereby increased Angiotensin II plasma level (Fig. 4D). Angiotensin II has induced monocytic ROS production (Fig. 1, B and C) responsible for DNA damage in T cells (Fig. 3B). At that time, T lymphocytes are possibly trying to repair this damage, an hypothesis accounting for the fact that the lymphopenia is not yet major. In this scenario, it is only a few days later that the consequence of this irreparable injury would appear clearly; lymphopenia in ICU patients who are at Day 12 of the disease (Table 1). In ICU patients, ROS expression was less intense than in non-ICU patients, probably due to the lower AngII plasma level in the former than in the latter. This decrease in AngII concentration over time might be the consequence of the increase in ACE2 expression reported in severe COVID-19 (18), driven by interferon (19), and/or reoxygenation (20), as well as the decrease in viral load (28). The amount of ROS released by monocytes would then be insufficient to provoke T cell apoptosis.

ROS-induced PBMC programmed cell death may have various deleterious effects. First, it may result in an immune deficiency favoring coinfections with other viruses (29), bacteria (30) or mycoses (31), and in a poor immunological memory paving the way for SARS-CoV-2 reinfection. Second, regulatory T-cell apoptosis may account for the Treg deficiency observed in severe forms of COVID-19 (32), favoring immune activation. Third, CD8+ T-cell and NK cell loss due to programmed cell death might contribute to a cytokine storm. Indeed, these cytotoxic lymphocytes have been found to be involved in the downregulation of immune activation in the course of infections via their ability to kill T-cells, NK, and antigen presenting cells (33, 34). Accordingly, in primary hemophagocytic lymphohistiocytosis, mutations resulting in cytolytic deficiency may provoke cytokine storms (35). Thus, the programmed death of CD8+ T-cells and NK cells could impair a negative feedback on immune activation. Fourth, CD4+ T lymphocyte apoptosis, particularly follicular helper T- cell apoptosis which may account for the depletion of this subpopulation (36) might explain the poor isotype switch and B memory observed in severe forms (37).

The release of ROS could have direct effects in addition to these indirect effects. As ROS are known to activate the pro-inflammatory transcription factor NFkB (38) and the NLRP3 inflammasome (39), they could favor a cytokine storm in severe forms. Locally, the numerous monocytes/macrophages in the low respiratory tract could also participate in endothelial cell, alveolar and vascular damage via ROS (40).

As we found, *in vitro*, that ROS released by COVID-19 monocytes induce DNA damage and apoptosis, as the proportion of DNA-damaged PBMCs we measured in patients correlated with their lymphopenia (a major pronostic marker in COVID-19), and as we found a link between the level of monocytic ROS expression in ICU patients and their survival, our data and the well-

documented proinflammatory effect of ROS argue for a role of this pathogenic pathway in the outcome of this disease. They could explain also why older people, males, patients with diabetes or prior cardiovascular diseases, who express low levels of ACE2 (41), present more often severe forms of COVID-19.

The mechanism we uncovered may also explain why SARS-CoV-2 variants with an enhanced affinity for their ACE2 receptor may be more pathogenic. Actually, these variants should provoke an increased ACE2 internalization, a higher level of AngII, a greater monocytic ROS production, and thereby more inflammation and more DNA damage resulting in lymphopenia and immune deficiency.

From a therapeutic viewpoint, our data may explain the beneficial effects of AT1 antagonists (42) and antioxidants (43) on COVID-19 observed in certain clinical trials. Given all the potential consequences of ROS release in severe COVID-19, therapeutic strategies aimed at reducing AngII signaling via AT1, ROS production, and apoptosis deserve more consideration (Fig. S1).

Acknowledgments

We are grateful to the persons who volunteered for this study, to Teresa Sawyers for the critical reading of the manuscript, to the biological resource center of the Nîmes University Hospital, and to BioMedTech core Facilities for their help with flow cytometry (INSERM US36, CNRS UMS2009, Paris, France).

References

1. Zhou F, Yu T, Du R, Fan G, Liu Y, Liu Z, et al. Clinical course and risk factors for mortality of adult inpatients with COVID-19 in Wuhan, China: a retrospective cohort study. Lancet. 2020;395(10229):1054-62.

2. Zhang X, Tan Y, Ling Y, Lu G, Liu F, Yi Z, et al. Viral and host factors related to the clinical outcome of COVID-19. Nature. 2020;583(7816):437-40.

3. Fan BE, Chong VCL, Chan SSW, Lim GH, Lim KGE, Tan GB, et al. Hematologic parameters in patients with COVID- 19 infection. Am J Hematol. 2020;95(6):E131-E4.

4. Reshi ML. RNA Viruses: ROS-Mediated Cell Death. Int J Cell Biol. 2014;2014:467452.

5. Casola A, Burger N, Liu T, Jamaluddin M, Brasier AR, Garofalo RP. Oxidant tone regulates RANTES gene expression in airway epithelial cells infected with respiratory syncytial virus role in viral-induced interferon regulatory factor activation. J Biol Chem. 2001;276(23):19715-22.

6. Hosakote YM, Jantzi PD, Esham DL, Spratt H, Kurosky A, Casola A, et al. Viral-mediated inhibition of antioxidant enzymes contributes to the pathogenesis of severe respiratory syncytial virus bronchiolitis. Am J Resp Crit Care Med 2011;183(11):1550-60.

7. Li Q, Wang L, Dong C, Che Y, Jiang L, Liu L, et al. The interaction of the SARS coronavirus non-structural protein 10 with the cellular oxido-reductase system causes an extensive cytopathic effect. J Clin Virol 2005;34(2):133-9.

8. Vijay R, Hua X, Meyerholz DK, Miki Y, Yamamoto K, Gelb M, et al. Critical role of phospholipase A2 group IID in age-related susceptibility to severe acute respiratory syndrome-CoV infection. J Exp Med. 2015;212(11):1851-68.

9. Codo AC, Davanzo GG, Monteiro LB, de Souza GF, Muraro SP, Virgilio-da-Silva JV, et al. Elevated Glucose Levels Favor SARS-CoV-2 Infection and Monocyte Response through a HIF-1alpha/Glycolysis-Dependent Axis. Cell Metab. 2020;32(3):437-46 e5.

10. Violi F, Oliva A, Cangemi R, Ceccarelli G, Pignatelli P, Carnevale R, et al. Nox2 activation in Covid-19. Redox Biol. 2020;36:101655.

11. Moghaddam A, Heller RA, Sun Q, Seelig J, Cherkezov A, Seibert L, et al. Selenium Deficiency Is Associated with Mortality Risk from COVID-19. Nutrients. 2020;12(7).

12. Thomas T, Stefanoni D, Reisz JA, Nemkov T, Bertolone L, Francis RO, et al. COVID-19 infection alters kynurenine and fatty acid metabolism, correlating with IL-6 levels and renal status. JCI Insight. 2020;5(14).

13. Darzynkiewicz Z, Zhao H, Halicka HD, Rybak P, Dobrucki J, Wlodkowic D. DNA damage signaling assessed in individual cells in relation to the cell cycle phase and induction of apoptosis. Crit Rev Clin Lab Sci. 2012;49(5-6):199-217.

14. Valdiglesias V, Giunta S, Fenech M, Neri M, Bonassi S. GammaH2AX as a marker of DNA double strand breaks and genomic instability in human population studies. Mutation Res. 2013;753(1):24-40.

15. Panier S, Boulton SJ. Double-strand break repair: 53BP1 comes into focus. Nature reviews Molecular cell biology. 2014;15(1):7-18.

16. Xavier LL, Ribas Neves PF, Paz LV, Neves LT, Bagatini PB, Saraiva Macedo Timmers LF, et al. Does Angiotensin II Peak in Response to SARS-CoV-2? Front Immunol. 2021;11:577875.

17. Chen Y, Zhang A-H, Huang S-M, Ding G-X, Zhang W-Z, Bao H-V, et al. NADPH oxidase-derived reactive oxygen species involved in angiotensin II-induced monocyte

chemoattractant protein-1 expression in mesangial cells. Zhonghua Bing Li Xue Za Zhi 2009;38(7):456-61.

18. Amati F, Vancheri C, Latini A, Colona VL, Grelli S, D'Apice MR, et al. Expression profiles of the SARS-CoV-2 host invasion genes in nasopharyngeal and oropharyngeal swabs of COVID-19 patients. Heliyon. 2020;6(10):e05143.

19. Ziegler CGK, Allon SJ, Nyquist S, Mbano IM, Miao VN, Tzouanas CN, et al. SARS-CoV-2 receptor ACE2 is an interferon-stimulated gene in human airway epithelial cells and is detected in specific cell subsets across tissues Cell. 2020;181(5):1016-35.

20. Wing PAC, Keeley TP, Zhuang X, Lee JY, Prange-Barczynska M, Tsukuda S, et al. Hypoxic and pharmacological activation of HIF inhibits SARS-CoV-2 infection of lung epithelial cells Cell Rep 2021;35(3):109020.

21. Andre S, Picard M, Cezar R, Roux-Dalvai F, Alleaume-Butaux A, Soundaramourty C, et al. T cell apoptosis characterizes severe Covid-19 disease. Cell Death Differ. 2022.

22. Tsuruya K, Tokumoto M, Ninomiya T, Hirakawa M, Masutani K, Taniguchi M, et al. Antioxidant ameliorates cisplatin-induced renal tubular cell death through inhibition of death receptor-mediated pathways. Am J Physiol Renal Physiol. 2003;285(2):F208-18.

23. Denning TL, Takaishi H, Crowe SE, Boldogh I, Jevnikar A, Ernst PB. Oxidative stress induces the expression of Fas and Fas ligand and apoptosis in murine intestinal epithelial cells. Free Radic Biol Med. 2002;33(12):1641-50.

24. Wang G, Jiang L, Song J, Zhou SF, Zhang H, Wang K, et al. Mipu1 protects H9c2 myogenic cells from hydrogen peroxide-induced apoptosis through inhibition of the expression of the death receptor Fas. Int J Mol Sci. 2014;15(10):18206-20.

25. Facchinetti F, Furegato S, Terrazzino S, Leon A. H(2)O(2) induces upregulation of Fas and Fas ligand expression in NGF-differentiated PC12 cells: modulation by cAMP. J Neurosci Res. 2002;69(2):178-88.

26. Montes-Berrueta D, Ramirez L, Salmen S, Berrueta L. Fas and FasL expression in leukocytes from chronic granulomatous disease patients. Invest Clin. 2012;53(2):157-67.

27. De Zio D, Cianfanelli V, Cecconi F. New insights into the link between DNA damage and apoptosis. Antioxid Redox Signal. 2013;19(6):559-71.

28. Boef AGC, van Wezel EM, Gard L, Netkova K, Lokate M, van der Voort PHJ, et al. Viral load dynamics in intubated patients with COVID-19 admitted to the intensive care unit. J Crit Care. 2021;64:219-25.

29. Abouelkhair MA. Non-SARS-CoV-2 genome sequences identified in clinical samples from COVID-19 infected patients: Evidence for co-infections. PeerJ. 2020;8:e10246.

30. Rodriguez-Nava G, Yanez-Bello MA, Trelles-Garcia DP, Chul Won Chung CW, Goar Egoryan G, Harvey J Friedman HJ. A Retrospective Study of Coinfection of SARS-CoV-2 and Streptococcus pneumoniae in 11 Hospitalized Patients with Severe COVID-19 Pneumonia at a Single Center. Med Sci Monit. 2020;26:e928754.

31. Segrelles-Calvo G, de S Araújo GR, Frases S. Systemic mycoses: a potential alert for complications in COVID-19 patients. Future Microbiol. 2020;15:1405-13.

32. Meckiff BJ, Ramírez-Suástegui C, Fajardo V, Chee SJ, Kusnadi A, Simon H, et al. Imbalance of Regulatory and Cytotoxic SARS-CoV-2-Reactive CD4 + T Cells in COVID-19. Cell. 2020;183:1-14.

33. Crouse J, Bedenikovic G, Wiesel M, Ibberson M, Xenarios I, Von Laer D, et al. Type I interferons protect T cells against NK cell attack mediated by the activating receptor NCR1. Immunity. 2014;40(6):961-73.

34. Madera S, Rapp M, Firth MA, Beilke JN, Lanier LL, Sun JC. Type I IFN promotes NK cell expansion during viral infection by protecting NK cells against fratricide. The Journal of experimental medicine. 2016;213(2):225-33.

35. Soy M, Atagündüz P, Atagündüz I, Sucak GT. Hemophagocytic lymphohistiocytosis: a review inspired by the COVID-19 pandemic. Rheumatol Int. 2021;41(1):7-18.

36. Duan Y-Q, Xia M-H, Ren L, Zhang Y-F, Ao Q-L, Xu S-P, et al. Deficiency of Tfh Cells and Germinal Center in Deceased COVID-19 Patients. Curr Med Sci 2020;40(4):618-24.

37. Newell KL, Clemmer DC, Cox JB, Kayode YI, Zoccoli-Rodriguez V, Taylor HE, et al. Switched and unswitched memory B cells detected during SARS-CoV-2 convalescence correlate with limited symptom duration medRxiv. 2020:2020.09.04.20187724.

38. Morgan MJ, Liu Z-G. Crosstalk of reactive oxygen species and NF-κB signaling. Cell Res. 2011;21(1):103-15.

39. Harijith A, Ebenezer DL, Natarajan V. Reactive oxygen species at the crossroads of inflammasome and inflammation. Front Physiol. 2014;5:352.

40. Rendeiro AF, Ravichandran H, Bram Y, Salvatore S, Borczuk A, Elemento O, et al. The spatio-temporal landscape of lung pathology in SARS-CoV-2 infection. medRxiv. 2020:2020.10.26.20219584.

41. Verdecchia P, Cavallini C, Spanevello A, Angeli F. The pivotal link between ACE2 deficiency and SARS-CoV-2 infection. Eur J Intern Med. 2020;76:14-20.

42. Saavedra JM. Angiotensin Receptor Blockers Are Not Just for Hypertension Anymore. Physiology (Bethesda). 2021;36(3):160-73.

43. Mohanty RR, Padhy BM, Das S, Meher BR. Therapeutic potential of N-acetyl cysteine (NAC) in preventing cytokine storm in COVID-19: review of current evidence. Eur Rev Med Pharmacol Sci. 2021;25(6):2802-7.

Figure legends

Figure 1. The monocytes from certain COVID-19 patients spontaneously produce ROS. (A) Fluorescence in monocytes from a healthy donor, pre-incubated (DPI + LPS, ---) or not (LPS, —) with DPI, exposed to DCFH-DA, and stimulated with lipopolysaccharide. As negative controls, fluorescence in the same monocytes pre-incubated (DPI, ···) or not (None, ···) with NADPH oxidase inhibitor DPI and exposed to DCFH-DA was analyzed. (B) Fluorescence in monocytes from a healthy donor (HD, ···), a non-ICU patient (non-ICU, —), and an ICU patient (ICU, ---) exposed to DCFH-DA. (C) Mean fluorescence intensity of ROS-producing monocytes from healthy donors (HD), non-ICU patients (non-ICU), and ICU patients (ICU) exposed to DCFH-DA. One-way ANOVA test $p < 0.001$. (D) Mean fluorescence intensity of ROS-producing monocytes from ICU patients who survived or not. (E) Identification of the classical, intermediate, and alternative monocyte subpopulations by flow cytometry. (F) Fluorescence in CD14hiCD16lo (---), CD14+CD16+ (—), and CD14loCD16hi (···) monocytes from an ICU patient exposed to DCFH-DA. (G) Percentages of CD14-CD16+ monocytes circulating in healthy (HDs), ICU and non-ICU donors. One-way ANOVA test $p = 0.032$. (H) Correlation between the proportions of intermediate and ROS-producing monocytes in ICU and non-ICU patients.

Figure 2. COVID-19 patient monocytes may induce DNA damage via ROS. (A) Detection of γ–H2AX foci by immunofluorescence in BJ cells co-cultured with PBMCs from a healthy donor or from a COVID-19 patient. Healthy donor's PBMCs treated with camptothecin were used as positive controls. (B) Quantification of the γ–H2AX foci induced in BJ fibroblasts by PBMCs from COVID-19 patients. The proportion of BJ cells presenting at least 5 foci per nucleus was quantified under microscopy. Each point represents one microscope field. Welch ANOVA test p

< 0.001. (C) γ–H2AX foci induced in BJ cells by COVID-19 patient's PBMCs are prevented by pre-incubating PBMCs with N-acetylcysteine (NAC) or diphenyleneiodonium (DPI). Each point represents one microscope field. Kruskal-Wallis test $p < 0.001$. (D) Monocytes isolated from the PBMCs of a COVID-19 patient are able to induce DNA damage in BJ cells. The ability to induce γ–H2AX foci in the BJ fibroblasts of PBMCs from a COVID-19 patient, of the same PBMCs depleted of monocytes, and of monocytes isolated from these PBMCs was tested. Each point represents one microscope field. Kruskal-Wallis test $p < 0.001$. (E) Intensity of phosphatidylserine expression at the surface of healthy donor PBMCs cocultured with non-ICU PBMCs able to induce DNA damage treated (non-ICU + NAC) or not (non-ICU) with N-acetylcysteine, or with ICU PBMCs unable to induce DNA damage treated (ICU + NAC) or not (ICU) with N-acetylcysteine, as detected by flow cytometry at day 6. Healthy donor PBMCs co-cultured with another healthy donor PBMCs (HD) or treated with lipopolysaccharide (HD + LPS) were used as negative and positive controls, respectively. One-way ANOVA test $p = 0.002$. (F) Intensity of phosphatidylserine expression at the surface of healthy donor PBMCs cocultured with COVID-19 monocytes able (patient 3) or not (patient 4) to induce DNA damage and treated (+ DPI) or not with DPI, as detected by flow cytometry at day 6. Camptothecin was used as a positive control.

Figure 3. DNA damage in COVID-19 PBMCs. (A) PBMCs from a COVID-19 patient whose monocytes induce DNA damage in bystander BJ cells spontaneously present with γ–H2AX foci. PBMCs from a healthy donor treated or not with camptothecin were used as positive and negative controls, respectively. (B) Percentages of PBMCs harboring γ–H2AX foci in healthy donors (HD), non-ICU patients (non-ICU), and ICU patients (ICU). Kruskal-Wallis test $p = 0.002$. (C) PBMCs from a COVID-19 patient whose monocytes induce DNA damage in

592 bystander BJ cells spontaneously present with 53BP1 foci. PBMCs from a healthy donor treated
593 or not with camptothecin were used as positive and negative controls, respectively. (D) Annexin
594 V expression on peripheral blood CD4+ T-cells and CD8+ T-cells of healthy donors (HD), non-
595 ICU patients (non-ICU), and ICU patients (ICU). One-way ANOVA test $p < 0.001$ for CD4+ T-
596 cells and $p < 0.001$ for CD8+ T-cells. (E) Correlation between the intensity of DNA damage in
597 PBMC and lymphocyte counts. The intensity of DNA damage in PBMCs is expressed as the
598 ratio (% patient PBMCs presenting γ–H2AX foci) : (% HD PBMCs presenting γ–H2AX foci).
599 **Figure 4. Angiotensin II induces ROS monocytic production and DNA damage.** (A)
600 Fluorescence in monocytes from a healthy donor, pre-incubated or not (···) with LPS (---) or
601 AngII (—), and exposed to DCFH-DA. (B) Fluorescence in monocytes from a healthy donor,
602 pre-incubated or not (···) with AngII (—) or with DPI and AngII (---), and exposed to DCFH-DA.
603 (C) Fluorescence in monocytes from a healthy donor, pre-incubated or not (···) with AngII (—),
604 or with losartan and AngII (---), and exposed to DCFH-DA. (D) Plasma levels of AngII in
605 patients and controls. Kruskal-Wallis test $p = 0.001$. (E) Correlation between plasma levels of
606 AngII and mean fluorescence intensity of ROS-producing monocytes exposed to DCFH-DA in
607 patients and controls. (F, G, H) AngII-activated monocytes induce DNA damage in
608 neighbouring cells. Ability of healthy donor monocytes stimulated (Monocytes/AngII) or not
609 (Monocytes) by AngII to cause γ-H2AX foci in bystander BJ cells (F, G) and HD PBMCs (H).
610 The effect or DPI (Monocytes/DPI+AngII, f) or AT1 antagonist (Monocytes/anti-AT1+AngII, g)
611 preincubation on the ability of AngII-stimulated monocytes to induce DNA damage is shown. BJ
612 cells (F, G) or PBMCs (H) exposed to camptothecin were used as a positive control
613 (Camptothecin). F, Welch ANOVA $p < 0.001$; G and H, Kruskal-Wallis test $p < 0.001$. (I)
614 Correlation between plasma levels of AngII and the ability of patient PBMCs to induce γ–H2AX

615 foci in bystander BJ cells. This ability is expressed as the ratio (% BJ cells presenting γ–H2AX
616 foci in presence of patient PBMCs) : (% BJ cells presenting γ–H2AX foci in presence of HD
617 PBMCs). (J) Correlation between mean fluorescence intensity of ROS-producing monocytes
618 exposed to DCFH-DA and the percentage of T lymphocytes expressing Fas.